State Modeling of the Land Mobile Satellite Channel Via an Image-Based Approach

Marie Rieche, Daniel Arndt, Alexander Ihlow and Giovanni Del Galdo

Digital Broadcasting Research Laboratory

Ilmenau University of Technology

Ilmenau, Germany

Abstract—This contribution investigates the image-based characterization of the land mobile satellite (LMS) channel. For a comprehensive multi-satellite model, a traditional measurement-based approach is not feasible due to the lack of available satellites at all possible orbital positions. To overcome this challenge, we propose to derive the LMS channel state-model from an evaluation of hemispheric images of the environment. With geometric considerations we can predict the position of an arbitrary satellite within the image. Based on this information the reception state of the LMS channel can be extracted. We determine the accuracy of our method by comparing it with results from RF (Radio Frequency) measurements and analyze it for various environments.

Index Terms—propagation; channel modeling; land mobile satellite channel; measurements; image processing

I. Introduction

Satellite broadcasting systems employing mobile receivers are increasingly popular, for example the Satellite Digital Audio Radio Service (SDARS) in the U.S. (Sirius XM Radio) [1], [2]. To design such systems an adequate description of the underlying radio propagation channel is essential.

The majority of statistical models for the land mobile satellite (LMS) link are based on a characterization of the signal power variations by measurements [3], [4]. Widely adopted is the characterization of the LMS channel on the basis of a sequence of reception states. In the literature, several statistical LMS models incorporating three states (line-of-sight, shadowing, blockage) [5]. Available 2-state-models ([6], [7]) are describing the channel as either *good* (*LoS/ light shadowing*) or *bad* (*NLoS/ heavy shadowing*). Deriving these models from signal measurements raises two main issues: First, it requires a high transmit power satellite already in orbit. Second, these measurements represent only one possible realization of the satellite position in azimuth and elevation. Moreover, the evaluation of modern transmission modes incorporating multi-satellite needs several satellites available to be measured simultaneously.

Another promising method of characterizing the LMS channel is an optical analysis of the environment [8]. By an optical analysis of the environment in fisheye images of the upper hemisphere the channel can be characterized [9]. In [10], the satellites visibility was compared with the measured power levels by optical inspection, already. The present contribution is about the extraction of the satellite reception states from images. The evaluation of this approach is performed from

the statistical channel modeling point of view. To verify the accuracy of our results, we compare them with results based on measured power levels, as a reference and present them for different environments. This paper is organized as follows: Section II describes the measurement validation campaign and data analysis. Subsequently, in Section III the statistics of the measured RF signal and the optical channel conditions are compared. Finally, Section IV concludes the paper.

II. Measurements and Data Analysis

A. Data Acquisition

To test an validate the proposed method we consider extensive measurements conducted in the context of the project Mobile satellite channeL with Angle DiversitY (MiLADY) [11]. In Figure 1, the traveled distance of 3700 km
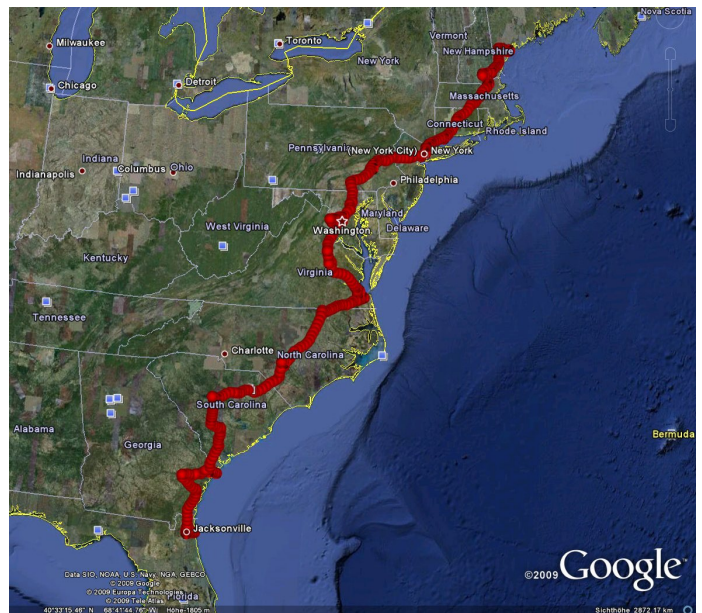

Fig. 1. Measurement campaign of about 3700 km along the east US coast.

along the east coast of the U.S. is shown. The measurement equipment synchronously recorded the received power levels of Sirius XM Radio, operating in the S-band at 2.3 GHz. This system consists of two geostationary (GEO) satellites and three highly elliptical orbit (HEO) satellites, where two of the three HEOs were always visible at the same time. The sampling rate

of the power levels was 2.1 kHz. The exact measuring time and vehicle position was logged via GPS. Moreover, a camera was mounted on the van to document the environmental conditions (5 frames per second with a resolution of 1024×768 pixels).

B. Image Analysis and State Identification

We characterize the LMS channel on the basis of a sequence of reception states consisting of *good* and *bad*, corresponding to the reception status *LoS / light shadowing* and *NLoS / heavy shadowing*, respectively [6], [7]. In this contribution we derive the LMS channel reception state from images of the environment. First of all, the hemispheric images are classified into *Sky* and *Object*. A possible implementation that models the color distributions of the classes as multivariate Gaussians and estimates the class parameters via the Expectation Maximization (EM) algorithm, is described in [12]. An example of this binary classification is depicted in Figure 2. In a second step, the conversion from the classified fisheye
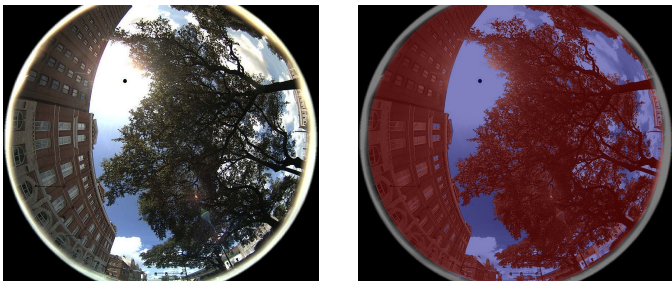

Fig. 2. The images show an exemplary hemispheric image (left) and the overlay of the binary classification into *Sky* and *Object* (right).

images to rectangular images in landscape panoramic form is performed, as you can see in Figure. The transformation is processed such that the output panoramic image is represented of a polar coordinate system, as you can see in Figure 3. Thus, objects appear less distorted. Additionally, the images are shifted based on the GPS heading information of the car, thus $0°$ corresponds to the north direction. Consequently, it is possible to choose any position in elevation and azimuth for arbitrary satellite constellations. By fusing the time and location information we determine the satellite positions in the binary images. The panoramic image can be used to derive
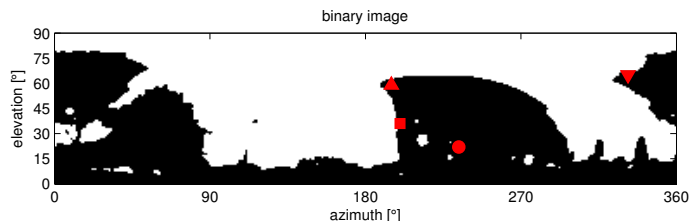

Fig. 3. The converted panoramic binary images are of size 90×360 pixels, where the resolution is one degree in elevation and in azimuth. The symbols show the positions of the four satellites (Sirius 1 ▲, Sirius 2 ▼, XM-3 ■ and XM-4 ●).

the reception state of satellites for any possible position. In order to validate our approach, we compare state sequences derived from images with states derived from RF signals. The state detection based on recorded satellite power levels is performed by global thresholding, as described in [13]. To derive state sequences from image data, the binary value from the panoramic image at a defined satellite position is taken, where white represents the *good* state and black the *bad* state.

III. RESULTS AND CONCLUSION

This paper considers RF and image state sequences referring to one day of measurements in the area of Portland, comprising the environments urban, suburban, commercial and highway. An accurate description of the given environment types can be found in [14]. For a preliminary optical evaluation we show in Figure 4, the actual RF signal level (blue solid line) and the corresponding binary image values (red circles) are compared as time series. Each satellite signal (Sirius 1, Sirius 2, XM-3 and XM-4) is plotted in a separate diagram, over a time period of approximately $2\,\mathrm{min}$. From the slow fading point of view, the binary values and the RF signal level are clearly in good agreement. Nevertheless, there are some parts which do not fit, such as in the first diagram from 15:01:07 till 15:01:15. Indeed, at this time the satellite position was at the edge of a building, which can cause erroneous identifications. Other possible reasons are e.g. windows in which the sky is mirrored and consequently they are incorrectly detected as sky. To verify the matching of the obtained RF and images states we determine a correlation factor. Let x_i and y_i be the state sequences from RF power levels and from images, respectively, both have the length N. x_i and y_i are $\in \{0, 1\}$, where "0" represents the *bad* state and "1" the *good*. The correlation factor $r_{xy} \in [\text{-}1, 1]$ is defined as

$$r_{xy} = \frac{1}{N} \sum_{x_i = y_i} 1 - \frac{1}{N} \sum_{x_i \neq y_i} 1 \quad \text{for} \ \ i = 1, .., N. \quad (1)$$

In Table I r_{xy} is presented for different satellites with different mean elevation angle ϕ and each for urban, suburban commercial and highway environment. There is a clear tendency of an increasing correlation r_{xy} associated with an increasing mean elevation angle ϕ. At high elevation angles (Sirius 1, Sirius 2) a clear LoS state is more probable. This leads to a more successful state identification, as shown by the higher correlation coefficient. For lower elevations, as (XM-3, XM-3) at $38°$ and $23°$, false detected windows and building edges are a problems to cope with (referring to Section II-B). The

TABLE I
MEAN ELEVATION ANGLE ϕ FOR THE DIFFERENT SATELLITES. FOR EACH, THE CORRELATION FACTOR r_{xy} BETWEEN THE STATE SEQUENCE OF RF x AND IMAGE DATA y IS OBTAINED.

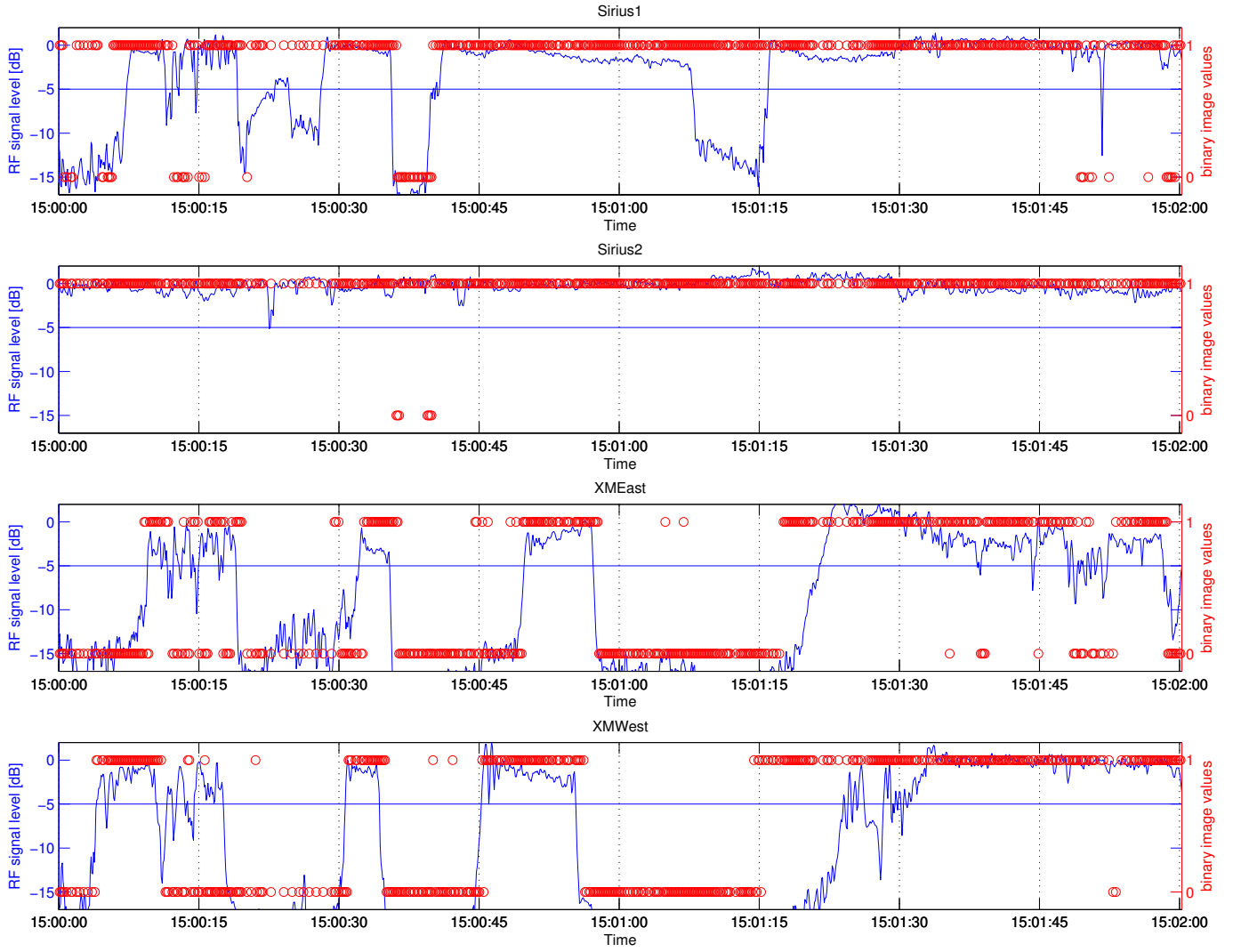|	Sirius 1	Sirius 2	XM-3	XM-4
ϕ	$65°$	$68°$	$38°$	$23°$
r_{xy} urban	0.91	0.92	0.75	0.79
r_{xy} suburban	0.72	0.79	0.57	0.53
r_{xy} commercial	0.98	0.98	0.82	0.89
r_{xy} highway	0.96	0.96	0.93	0.94

Fig. 4. The measured RF signal level (blue) and the corresponding binary values (red circles) are plotted for the XM-3 satellite over a certain time period ($\approx 2\,\mathrm{min}$). The horizontal line shows the threshold for state identification, which is 5dB below the LoS.

different types of environments achieve very sound results, with slightly higher correlations for commercial and highway, because of the lower height of objects. However, the worst case represents suburban environment. This is related to the huge number of trees right by the road. They lead to a *bad* state determined by the images, however the RF power does not decrease beyond the state detection threshold.

From the LMS channel modeling point of view, several statistical parameters need to be determined. Therefore, the evaluation is carried out in terms of state probabilities and state duration statistics. In Figure 5 is the *bad* state probability for Sirius 1, Sirius 2, XM-3 and XM-4 plotted, comparing the results of the RF and image (IM) based analysis. The respective results are also presented for the four types of environment.

Since only two states are assumed, the *bad* state probability is calculated using $P_{\mathrm{g}} = 1 - P_{\mathrm{b}}$.

Obviously, the *bad* state probability is lower for the HEO satellites (Sirius 1, Sirius 2), because of the higher elevation angles (see Table I). The probabilities for RF and image fit very well, only with slight deviations on average about 0.02. Sirius 1 in suburban environment represents the worst case with a deviation of 0.06 between image and RF. Again this refers to the different definition of the thresholds, where the binary image only distinguishes between clear LoS and everything which is left over. In comparison, the thresholding of the RF signal level at $5\,\mathrm{dB}$ below LoS corresponds more to the meaning *LoS/ light shadowing* and *NLoS/ heavy shadowing*. Especially the suburban environment is characterized by a high number of trees, which makes this effect visible.

Figure 6 shows the *bad* state probability P_{b} over the elevation angle ϕ for the environment types urban, suburban, commercial and highway. P_{b} is decreasing with the decreasing object height in the order of urban / suburban, commercial and highway. As expected the *bad* state probability P_{b} becomes zero for elevations approaching $90°$, besides the curve of
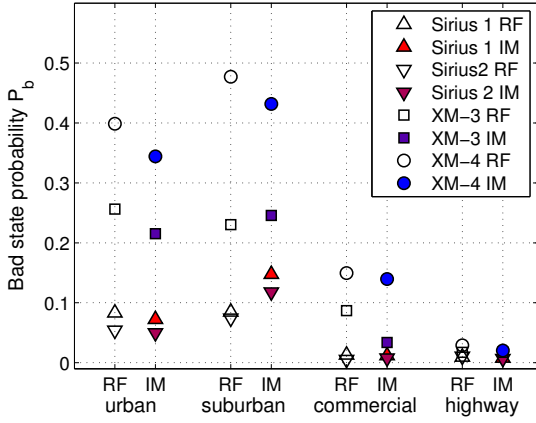
Fig. 5. The *bad* state probability P_b for each satellite, comparing the states derived from RF signal levels and binary image values in four different environments.
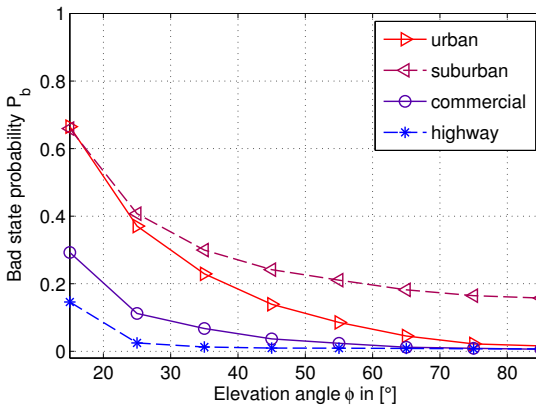

Fig. 6. The *bad* state probability P_b over the elevation angle ϕ for the environment types urban, suburban, commercial and highway.

suburban environment. The reason for that are the trees right by the road, which soar (reach) up into regions of high elevation.

The state duration statistics considering one measurement day (including the four environments) are presented for the four different satellites, all shown in Figure 7. In order to evaluate and analyze the matching of the generated RF and image states, we used the complementary cumulative distribution function. With respect to RF based states and image-based states the functions match very well for *good*, only with slight differences ($\leq 1\,\sec$).

IV. CONCLUSIONS

In this paper we present the characterization of the LMS channel via panoramic images transformed from fisheye images. To verify our approach we consider the corresponding measured RF signal levels, as a ground truth. Furthermore, we determined reception states to characterize various satellite links. As evaluation criteria we use a correlation factor, the bad state probability and the state duration statistics. They show a very good agreement between the RF-based and the image-
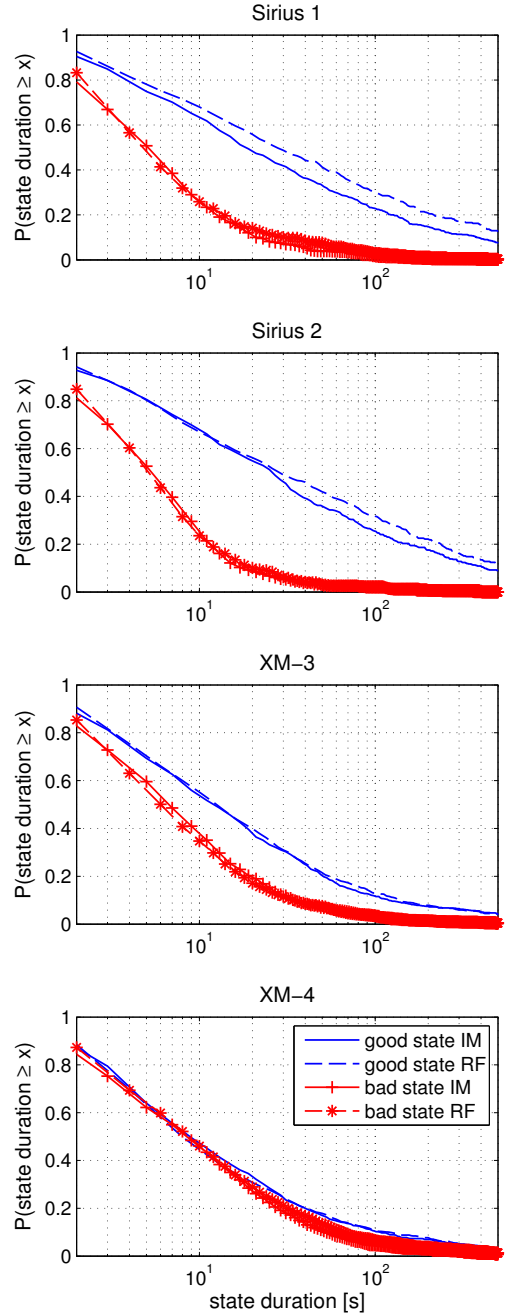

Fig. 7. State duration statistics for *good* (blue) and *bad* (red) state are presented for each satellite (Sirius 1, Sirius 2, XM-3 and XM-4). Additionally, they are analyzed for RF based states (dashed lines) and image (IM) based states (solid lines).

based results. The matching of the data decreases in suburban environment because of the high trees.

It is found that the optical approach can detect very slow-fading effects (states) reliably.

V. Acknowledgment

References

[1] R. Akturan, "An overview of the Sirius satellite radio system," *International Journal of Satellite Communications and Networking*, vol. 26, no. 5, pp. 349–358, 2008.

[2] R. A. Michalski, "An overview of the XM satellite radio system," in *20th AIAA International Communication Satellite Systems Conference and Exhibit*, May 2002.

[3] E. Lutz, D. Cygan, M. Dippold, F. Dolainsky, and W. Papke, "The land mobile satellite communication channel – recording, statistics, and channel model," *IEEE Transactions on Vehicular Technology*, vol. 40, no. 2, pp. 375–386, 1991.

[4] F. Pérez-Fontán, M. Vázquez-Castro, C. Enjamio Cabado, J. Pita García, and E. Kubista, "Statistical modeling of the LMS channel," *IEEE Transactions on Vehicular Technology*, vol. 50, no. 6, pp. 1549–1567, Nov. 2001.

[5] F. Pérez-Fontán, M. A. Vázquez-Castro, C. Enjamino, and J. P. García, "Comparison of generative statistical models for the LMS channel," in *IEEE 55th Vehicular Technology Conference, VTC Spring 2002*, vol. 2, 2002, pp. 871–875.

[6] R. Prieto-Cerdeira, F. Perez-Fontan, P. Burzigotti, A. Bolea-Alamañac, and I. Sanchez-Lago, "Versatile two-state land mobile satellite channel model with first application to DVB-SH analysis," *International Journal of Satellite Communications and Networking*, vol. 28, no. 5-6, pp. 291–315, 2010.

[7] E. Lutz, "A Markov model for correlated land mobile satellite channels," *International Journal of Satellite Communications*, vol. 14, pp. 333–339, 1996.

[8] R. Akturan and W. J. Vogel, "Photogrammetric mobile satellite service prediction," in *Proceedings of the Eighteenth NASA Propagation Experimenters Meeting (NAPEX XVIII) and the Advanced Communications Technology Satellite (ACTS) Propagation Studies Miniworkshop*, Vancouver, BC Canada, Jun. 1994, pp. 159–163.

[9] H.-P. Lin and W. J. Vogel, "Photogrammetric satellite service prediction in a roadside treeshadowing environment," in *Vehicular Technology Conference*, vol. 2, 1998, pp. 1485–1487.

[10] A. Ihlow, D. Arndt, F. Topf, C. Rothaug, T. Wittenberg, and A. Heuberger, "Photogrammetric satellite service prediction-correlation of RF measurements and image data," in *Broadband Multimedia Systems and Broadcasting (BMSB), 2011 IEEE International Symposium on*. IEEE, 2011, pp. 1–6.

[11] E. Eberlein, A. Heuberger, and T. Heyn, "Channel models for systems with angle diversity – The MiLADY project," in *ESA Workshop on Radiowave Propagation Models, Tools and Data for Space Systems*, Noordwijk, the Netherlands, Dec. 2008.

[12] A. Ihlow and A. Heuberger, "Sky detection in fisheye images for photogrammetric analysis of the land mobile satellite channel," in *Proceedings of the 10th Workshop Digital Broadcasting*, Ilmenau, Germany, Sep. 2009, pp. 56–60.

[13] D. Arndt, A. Ihlow, T. Heyn, A. Heuberger, R. Prieto-Cerdeira, and E. Eberlein, "State modelling of the land mobile propagation channel for dual-satellite systems," *EURASIP Journal on Wireless Communications and Networking*, vol. 2012, no. 1, p. 228, 2012.

[14] D. Arndt, A. Ihlow, A. Heuberger, T. Heyn, and E. Eberlein, "Land mobile satellite channel characteristics from the MiLADY project," in *Proceedings of the 10th Workshop Digital Broadcasting*, Ilmenau, Germany, Sep. 2009, pp. 49–55.